REMARKS

A Request For A Three Month Extension Of Time is submitted herewith

The Examiner has rejected Claim 60 and 61 under 35 U.S.C. 112, first paragraph, as failing to comply with the enablement requirement. Applicant has rewritten Claim 60 in independent form (it previously depended from Claim 59) to correct the indefiniteness and eliminate the requirement of a combined measurement through both the eye and the skin. Since Claim 61 depends from Claim 60, no amendment was felt necessary.

The examiner has rejected Claims 44-59 based on double patenting in view of U. S. Patent No. 6,246,893. The rejection for this statutory type (35 U.S.C. 101) double patenting rejection is based upon the Examiner's belief that the medical term "iris", to identify an element of the eye, by its structure is identical to the phrase "reflective interior surface" also to identify an element of the eye. Applicant has respectfully requested reconsideration of this rejection and in support thereof has submitted two published technical articles (Exhibits 1 and 2) supporting the position that other portions of the human eye, in addition to the iris, present reflective surfaces. In each of the attached technical papers, a discussion is presented of the reflective characteristics of at least the human lens and other "internal surface reflections". Accordingly, it is respectfully submitted that the statutory double patenting rejection is inappropriate and the claims incorporating the phrase "reflective interior surface" are distinguishable from those in the patent 6,246,893.

Claims 44-59 are also rejected for double patenting under the judicially created doctrine of obviousness-type double patenting in view of U. S. Patent No. 6,246,893. A Terminal Disclaimer in compliance with 37 C.F.R. 1.321(c) is submitted herewith to overcome the rejection on non-statutory double patenting.

In view of the above amendment and arguments, it is respectfully submitted that the present application is in condition for allowance and such allowance is earnestly solicited.

Respectfully submitted,

CAHILL, VON HELLENS & GLAZER P.L.C.

William C. Cahill
Registration No. 19,742

2141 East Highland Avenue
155 Park One
Phoenix, Arizona 85016
(602) 956-7000
Docket No. 5899-A-05

laboratory science

Intraocular lens surfaces and their relationship to postoperative glare

Jay C. Erie, MD, Mark H. Bandhauer, MS

Purpose: To estimate the potential for surface reflections in recently introduced intraocular lenses (IOLs) and to determine optic surface designs that will reduce surface reflections.

Setting: Mayo Clinic, Rochester, Minnesota, USA.

Methods: Surface-reflected glare in the unaccommodated human crystalline lens and in 6 IOLs (Bausch & Lomb SoFlex® LI61U, Pharmacia CeeOn® 911A, Allergan Sensar® AR40, Bausch & Lomb Hydroview® H60M, Alcon AcrySof® MA60BM, Alcon AcrySof SA30AL) was examined in a physiologic eye model using the ZEMAX optical design program. Internal and external surface reflections were described and compared in terms of IOL surface reflectivity (%), area of the reflected glare image (mm²), and relative intensity of the reflected glare image.

Results: Compared to surface reflections from the unaccommodated human lens with a corneal power of 43.0 diopters, all the IOLs increased the relative intensity of internal and external reflections by 3- to 36-fold except the MA60BM and the SA30AL, which increased the relative intensity of internal and external reflections by 730- to 1090-fold.

Conclusions: All the IOLs studied variably increased internal and external surface reflections when compared to the human crystalline lens. Surface reflections were minimized in optic designs with an anterior radius of curvature of approximately 17.0 mm or less.

J Cataract Refract Surg 2003; 29:336–341 © 2003 ASCRS and ESCRS

Various clinical reports have shown that patients who receive intraocular lenses (IOLs) occasionally experience some degree of glare, arcs, or halos after cataract surgery.[1,2] These undesirable optical effects have been referred to as photic phenomena,[1] undesired light images,[3] and pseudophakic dysphotopsia.[2,4–7] In most cases, postoperative dysphotopsia phenomena are without significant consequences and resolve quickly and spontaneously.[1] Recent clinical reports[4–7] and surveys,[8,9] however, have found pseudophakic dysphotopsia to be a common reason for explantation of certain acrylic IOLs.

Pseudophakic dysphotopsia has been attributed to edge glare[2,3,10] and surface reflections.[11] It is thought that edge glare is caused by the internal reflections from a truncated IOL edge, whereas surface reflections are caused by a high-refractive-index optic material combined with a relatively flat anterior IOL surface. Recently, new IOLs have become available that are composed of different materials and have new optic surface designs. These IOL materials and optic design modifications may reduce the prevalence of pseudophakic dysphotopsia.

Because our first paper on IOL reflections suggests that optic material reflectivity may be the lesser contributor to surface glare,[11] the main question remains whether surface curvature combinations in newer IOLs are adequate to reduce the potential for surface reflec-

EXHIBIT 1

Amendment to Serial No. 09/878,307 entitled "Method and Device for Glucose Concentration Measurement With Special Attention to Blood Glucose Determinations"

tions. In this study, we further evaluated surface reflections in recently introduced IOLs, compared them to the unaccommodated human crystalline lens as a new standard of low glare, and determined specific IOL anterior surface curvatures that will minimize surface reflections.

## Materials and Methods

Materials

The IOLs studied were the Bausch & Lomb SoFlex® LI61U (equi-biconvex design; silicone refractive index [RI], 1.43; anterior radius of curvature [ARC], 10.0 mm), Pharmacia CeeOn® 911A (equi-biconvex; silicone RI, 1.46; ARC, 13.0 mm), Bausch & Lomb Hydroview® H60M (equi-biconvex; hydrogel RI, 1.474; ARC, 14.0 mm), Allergan Sensar® AR40 (equi-biconvex; acrylic RI, 1.47; ARC, 15.0 mm), Alcon AcrySof® MA60BM (unequal biconvex; acrylic RI, 1.55; ARC, 32.0 mm), and Alcon AcrySof SA30AL (unequal biconvex; acrylic RI, 1.55; ARC, 21.0 mm). The unaccommodated human crystalline lens was based on Helmholz[12] schematic values (unequal biconvex; cortex RI, 1.386; ARC, 10.0 mm) so that all samples were a consistent optical power of 19.0 diopters (D).

The formation of surface-reflected glare images by the IOLs and the human lens was evaluated by modeling the light source, the eye, and the human lens or IOL using the ZEMAX optical design program (Focus Software Inc.) as described previously.[11] Briefly, the external light source consisted of collimated light at 2.5 degrees to the optical axis (chosen to separate the glare image from the main image rays). A physiologic eye model was designed with the following physiological parameters: corneal power, 38.0 D, 40.0 D, 43.0 D, 46.0 D, and 48 D; anterior chamber depth, 4.5 mm; approximate axial length, 23.5 mm; IOL power, 19.0 D; optic diameter, 5.5 to 6.0 mm; pupil diameter, 3.2 to 3.8 mm.

Reflections and Optical Analysis

Reflections at the anterior surface of the human lens or IOL were determined using a previously described optical design program and classic optical surface analysis.[11] The reflectivity of light at normal incidence was calculated for each material.[13]

To evaluate external surface reflections, the optical design program traced rays from the glare source, through the cornea, to the anterior surface of the human lens or IOL, and back to an outside observer (Figure 1). Previous ray-tracing work has shown that the external surface reflections from the IOL anterior surface, rather than the posterior surface, are responsible for reflected glare.[11] The area (mm²) of the reflected external image 1 m from the phakic or pseudophakic eye was ratioed to the area of the observer's pupil to obtain a relative area value. (A typical area of 8.0 mm² for a 3.2 mm pupil was used.) The
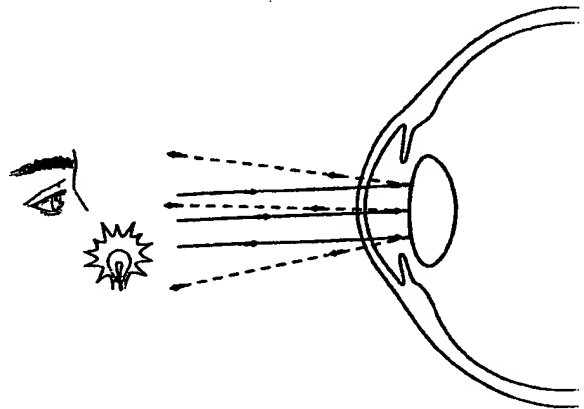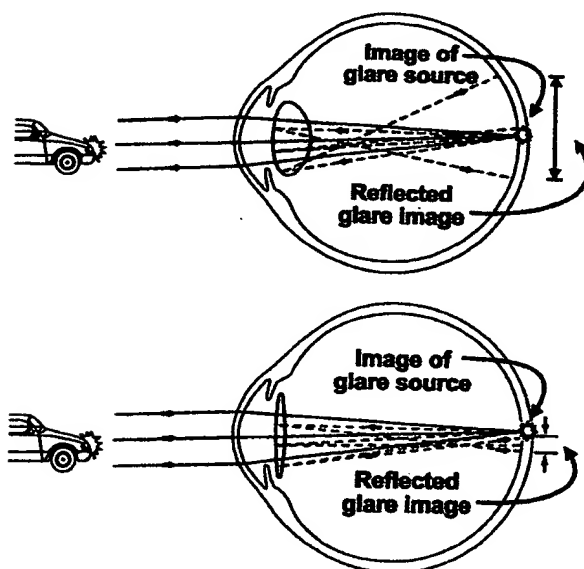

Figure 1. (Erie) External surface reflections. The unaccommodated human crystalline lens has a steep anterior radius of curvature (10.0 mm) that acts as a partially reflecting convex mirror, producing reflected light rays that are highly divergent. The low-RI human lens material also has low reflectivity. As a result of these characteristics, the external glare image is of low intensity.

ratio was multiplied by relative reflectivity ($r/r_{human\ lens}$) to obtain the relative ratio for external glare.[11]

To evaluate internal surface reflections, the optical design program traced rays from the external light source, through the human lens or IOL, and to the retina. It is known that the human fundus acts as a diffuse reflector and that as much as 75% of light focused on the fundus is reflected anteriorly.[14,15] Fundus reflectivity is the basis for ophthalmoscopy. Therefore, fundus reflections were hypothesized as the glare point source, assuming an emmetropic eye. The rays reflected from the fundus were traced back to the anterior surface of the human lens or IOL, which acts as a partially reflecting mirror that is concave from the inside, where they were again reflected back to the retina (Figure 2). Previous ray-tracing has shown that internal reflections from the convex posterior surface of the lens do not contribute to reflected glare as these reflections are markedly divergent and of low intensity.[11] The area (mm²) of the focused or defocused internal glare image at the curved retinal surface from the double reflection was then calculated using spot diagrams. The relative intensity of the internally reflected glare image was described and compared in terms of a relative intensity ratio proportional to reflectivity (%)/area (mm²).[11]

The relative intensity ratio of the unaccommodated human lens (corneal power 43.0 D) was arbitrarily given a value of 1 for internal and external reflections. No specific value of fundus reflectivity was used as the analysis was limited to a comparison of surface reflectivity and subsequent glare image sizes in relative units only.

The relative intensity of IOL surface reflections varies with corneal power.[11] To determine an optic surface design with minimal potential for surface reflectivity, an optical de-

Figure 2. (Erie) Internal surface reflections. Anteriorly reflected light from the fundus (fundus reflectivity, hatched lines) can be redirected posteriorly by a reflection from the anterior surface of the human lens or IOL to form a reflected retinal glare image. *Top:* The unaccommodated human lens defocuses internal surface reflections to a large area that is of low intensity. *Bottom:* The highly reflective, flatter anterior surface of the AcrySof SA30AL IOL focuses internally reflected light rays near the retina, producing a glare image that is small in area but of high intensity.

sign program was used to calculate the relative intensity of surface reflections over a range of IOL anterior surface radii of curvature (10.0 to 32.0 mm) and corneal powers (38.0 to 48.0 D).

Results

The IOL surface reflectivity (%), the area of the reflected glare image (mm²), and the relative intensity ratio of the internal and external reflected glare image for the unaccommodated human lens and the IOLs are shown in Tables 1 and 2, respectively. The unaccommodated human lens defocused the internal and external reflected glare image to a large area that was of low intensity (Figures 1 and 2, top). Similar to the human lens, IOLs with a low anterior radius of curvature and composed of a low-RI material (SoFlex LI61U, CeeOn 911A, Sensar AR40, Hydroview H60M) defocused surface reflected light to a large area that was of low intensity (Tables 1 and 2). In contrast, IOLs with a high anterior radius of curvature and composed of a high-RI

material (AcrySof MA60BM and AcrySof SA30AL) focused surface reflected light to a small area that was of high intensity (Tables 1 and 2; Figure 2, *bottom*).

The relative intensity of internal surface reflections with respect to different corneal powers and different IOL anterior radii of curvature is shown in Figure 3. For all corneal powers, the relative intensity of surface reflections was minimized when the radius of curvature of the IOL anterior surface was approximately 17.0 mm or less.

Discussion

We used ray-tracing analysis to demonstrate that recently introduced IOLs variably increase internal and external surface reflections for all corneal powers when compared to the unaccommodated human crystalline lens. Our data suggest that IOL surface reflections can be minimized, however, by using an optic design with an anterior radius of curvature of approximately 17.0 mm or less.

The observed low value for internal and external surface reflections in our simulation of the unaccommodated human lens is validated by the lack of significant glare described by most humans without cataract formation. In contrast, 20% to 49% of pseudophakic patients with various IOL models describe some type of postoperative glare or light-related phenomenon that generally resolves quickly and spontaneously.[1,2] Our ray-tracing analysis showed that all the IOLs we studied variably increased the intensity of surface reflections. As a result, one might expect that some pseudophakic patients would notice light-related phenomena in the early postoperative period. The calculated intensity of internal and external surface reflections, however, varied by as much as 5000-fold depending on the optic material, the optic design, and the corneal power. Therefore, certain IOL optic designs appear to possess a greater potential for surface reflections that, in some people, may be intense enough to be persistent and clinically significant.

Reflections from an IOL can be projected internally or externally. External reflections from the anterior surface of an IOL have been shown to be the cause of the "flash" or "glint" seen in a pseudophakic eye by an outside observer.[11] The intensity or visibility of external surface reflections increases in IOLs composed of a reflective high-RI material combined with a flatter anterior surface curvature. The AcrySof MA series IOL

Table 1. External reflectivity, relative area, and relative intensity ratio of external glare image for observer 1 m from lens or IOL of 19.0 D.*

Optic Design	Optic Material (RI)	IOL Model	Reflectivity (%)	Corneal Power (D)	Relative Area of External Glare (mm²)	Relative Intensity Ratio
Human lens	Cortex (1.386)	Unaccommodated clear lens	0.03	48	10 800	1.3
			(decimal 0.000337)	46	12 000	1.2
				43	14 400	1.0
				40	16 900	0.9
				38	18 800	0.8
Equi-biconvex	Silicone (1.43)	Bausch & Lomb SoFlex L161U	0.11	48	11 600	4.2
				46	13 000	3.8
				43	15 400	3.2
				40	18 000	2.7
				38	20 000	2.4
Equi-biconvex	Silicone (1.46)	Pharmacia CeeOn 911A	0.19	48	3900	21.0
				46	4600	18.0
				43	5800	14.0
				40	7200	11.0
				38	8300	10.0
Equi-biconvex	Acrylic (1.47)	Allergan Sensar AR40	0.23	48	2500	40.0
				46	3000	33.0
				43	3900	25.0
				40	5000	19.0
				38	5900	16.0
Equi-biconvex	Hydrogel (1.474)	Bausch & Lomb Hydroview H60M	0.24	48	2100	50.0
				46	2500	41.0
				43	3400	30.0
				40	4400	23.0
				38	5200	20.0
Unequal biconvex	Acrylic (1.55)	Alcon AcrySof MA60BM	0.55	48	600	390.0
				46	430	540.0
				43	220	1090.0
				40	74	3200.0
				38	17	13 700.0
Unequal biconvex	Acrylic (1.55)	Alcon AcrySof SA30AL	0.55	48	47	5000.0
				46	120	1950.0
				43	320	730.0
				40	620	380.0
				38	900	260.0

RI = refractive index
*Incident light at 2.5 degrees to optical axis

incorporates both these features in its optic design. Our ray-tracing finding of increased visibility of external surface reflections with this IOL is consistent with the clinical reports of visible external reflections in these patients.[4–6]

In recent ray-tracing analyses, internal reflections from an IOL edge[10] or an IOL surface[11] have been suggested to be the cause of unwanted photic phenomena reported by some pseudophakic patients. A sharp, truncated IOL edge can produce a reflected arc-shaped glare image on the opposite side of the retina that is maximal when incident light is about 35 degrees to the optical axis.[10] An IOL with a nearly flat anterior surface curvature can produce an internal surface-reflected glare image that is round or oval, although the intensity is less as a result of double reflection.[11] In addition, the intensity of both edge- and surface-reflections is further increased by using a more reflective high-RI material such

Table 2. Internal reflectivity, area of retinal glare image, and relative intensity ratio at the retina for the unaccommodated human lens and various IOLs of 19.0 D power.*

| Optic Design	Optic Material (RI)	IOL Model	Reflectivity (%)	Corneal Power (D)	Area of Retinal Glare Image (mm²)	Relative Intensity Ratio
Human lens	Cortex (1.386)	Unaccommodated clear lens	0.03 (decimal 0.000337)	48	24.0	1.5
				46	28.0	1.3
				43	36.0	1.0
				40	45.0	0.8
				38	53.0	0.7
Equi-biconvex	Silicone (1.43)	Bausch & Lomb SoFlex L161U	0.11	48	20.0	6.1
				46	24.0	5.1
				43	31.0	3.9
				40	40.0	3.1
				38	47.0	2.6
Equi-biconvex	Silicone (1.46)	Pharmacia CeeOn 911A	0.19	48	6.8	30.0
				46	8.5	24.0
				43	12.1	17.0
				40	16.7	12.0
				38	21.0	10.0
Equi-biconvex	Acrylic (1.47)	Allergan Sensar AR40	0.23	48	4.2	58.0
				46	5.4	44.0
				43	8.1	30.0
				40	11.7	21.0
				38	14.9	16.0
Equi-biconvex	Hydrogel (1.474)	Bausch & Lomb Hydroview H60M	0.24	48	3.5	73.0
				46	4.6	56.0
				43	7.0	36.0
				40	10.3	25.0
				38	13.2	19.0
Unequal biconvex	Acrylic (1.55)	Alcon AcrySof MA60BM	0.55	48	1.30	460.0
				46	1.01	580.0
				43	0.58	1020.0
				40	0.24	2500.0
				38	0.07	8000.0
Unequal biconvex	Acrylic (1.55)	Alcon AcrySof SA30AL	0.55	48	0.04	14 000.0
				46	0.17	3500.0
				43	0.59	1000.0
				40	1.36	430.0
				38	2.20	270.0

RI = refractive index
*Incident light at 2.5 degrees to optical axis

as acrylic (RI 1.55), which has 5 times the reflectivity of low-index silicone (RI 1.43).[11,15] Clinical reports have primarily associated unwanted internal glare with IOLs that incorporate all 3 internal reflection risk factors (sharp edge, flat anterior surface, high-RI material) in the optic design.[4–7] As a result, it is unclear whether clinically significant pseudophakic dysphotopsia is due primarily to edge glare, surface glare, a combination, or another unexplained complex interaction in the pseudophakic visual system. In addition, it is not clear at what threshold edge- or surface-reflected light becomes clinically significant.

Nevertheless, as the expectations of patients and ophthalmologists increase after cataract surgery, it would be beneficial to minimize the external IOL surface reflections that are seen in the pseudophakic eye by an outside observer and the internal IOL surface reflections that are sometimes seen by the pseudophakic pa-
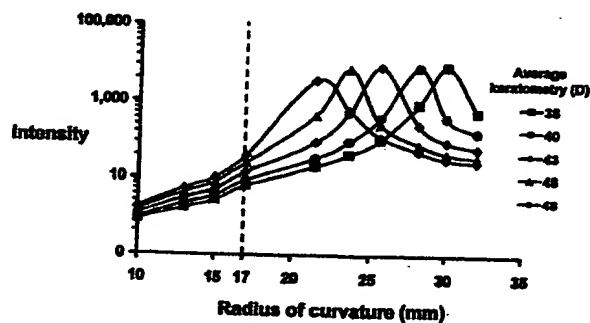
Figure 3. (Erie) The intensity of IOL surface reflections (relative to the unaccommodated human lens) as a function of corneal power and IOL anterior radius of curvature. For all corneal powers, the intensity of IOL surface reflections is minimized when the radius of curvature of the IOL anterior surface is approximately 17.0 mm or less (hatched line).

tient and described as dysphotopsia. These internal and external surface reflections are fundamentally related, and their intensity varies with corneal power and IOL anterior surface curvature.[11] Although this relationship is complex, our new ray-tracing data strongly suggest that potentially bothersome internal and external IOL surface reflections can be minimized for all corneal powers by using an optic design with an anterior radius of curvature of approximately 17.0 mm or less.

References

1. Arnold PN. Photic phenomena after phacoemulsification and posterior chamber lens implantation of various optic sizes. J Cataract Refract Surg 1994; 20:446–450

2. Tester R, Pace NL, Samore M, Olson RJ. Dysphotopsia in phakic and pseudophakic patients: incidence and relation to intraocular lens type. J Cataract Refract Surg 2000; 26:810–816

3. Masket S, Geraghty E, Crandall AS, et al. Undesired light images associated with ovoid intraocular lenses. J Cataract Refract Surg 1993; 19:690–694

4. Masket S. Consultation section; cataract surgical problem. J Cataract Refract Surg 1997; 23:979–984

5. Davison JA. Positive and negative dysphotopsia in patients with acrylic intraocular lenses. J Cataract Refract Surg 2000; 26:1346–1355

6. Farbowitz MA, Zabriskie NA, Crandall AS, et al. Visual complaints associated with the AcrySof acrylic intraocular lens. J Cataract Refract Surg 2000; 26:1339–1345

7. Hwang IP, Olson RJ. Patient satisfaction after uneventful cataract surgery with implantation of a silicone or acrylic foldable intraocular lens; comparative study. J Cataract Refract Surg 2001; 27:1607–1610

8. Mamalis N. Complications of foldable intraocular lenses requiring explantation or secondary intervention—1998 survey. J Cataract Refract Surg 2000; 26:766–772

9. Mamalis N. Explantation of intraocular lenses. Curr Opin Ophthalmol 2000; 11:289–295

10. Holladay JT, Lang A, Portney V. Analysis of edge glare phenomena in intraocular lens edge designs. J Cataract Refract Surg 1999; 25:748–752

11. Erie JC, Bandhauer MH, McLaren JW. Analysis of postoperative glare and intraocular lens design. J Cataract Refract Surg 2001; 27:614–621

12. Helmholtz H. Helmholtz's Treatise on Physiological Optics, translated from the German edition, edited by JPC Southall. New York, NY, Dover Publications, 1962; 382–400

13. Meyer-Arendt JR. Introduction to Classical and Modern Optics, 2nd ed. Englewood Cliffs, NJ, Prentice-Hall, 1984

14. Campbell FW, Gubisch RW. Optical quality of the human eye. J Physiol 1966; 186:558–578

15. Weale RA. Polarized light and the human fundus oculi. J Physiol 1966; 186:175–186

Real light scatter in the human crystalline lens

R.A. Weale

Department of Visual Science, Institute of Ophthalmology, University of London,
Judd Street, London, WC1H 9QS, England

Abstract. A comparison is made between the luminances of slit-lamp images of the normal human lens in frontal view with plane polarized light, when one ocular is provided with an analyzer and the other with variable neutral density filters, the light source being polarized perpendicularly to the direction of the analyzer. The amount of extinguished light is significantly larger as seen in the former, and rises systematically with age. The effect of varying the spectral composition of the illumination is also examined. What is conventionally referred to as scattered light appears to be made up of at least two separate components. The effect which this may have for our interpretation of pathological images is discussed.

Introduction

There is considerable interest in the extent of light scatter in the ocular lens for two reasons. First, it contributes to the impairment of the retinal image, thereby putting an upper limit on the optical resolving power of the eye. Secondly, it acts as an index of lenticular pathology, namely cataract. The experimental techniques used in these two categories differ. The former involves an objective or subjective assessment of the retinal image (Flamant 1955; Campbell and Robson 1968) or that formed by the lens on its own (Weale 1983). The latter is based on the use of the slit-lamp (cf. Niesel et al. 1976).

Allen and Vos (1967) and Sigelman et al. (1974) have given absolute values for the amounts of light scattered by various parts of the eye, and related them to ocular senescence. However, an important clinical dilemma remains unresolved. It is a matter of common experience that patients whose slit-lamp picture reveals the presence of considerable light-scatter nevertheless possess an all but normal or even unimpaired visual acuity (cf. Sigelman et al. 1974). Furthermore, the study by Zuckerman et al. (1973) with artificial cataracts showed that the optical performance of the lens suffers only with very "advanced" cataracts.

For the above reasons, and because scattered light has been used in an extensive series of calibrating studies of cataracts (cf. Lerman and Hockwin 1985), it is desirable to reconsider the problem.

The present experimental approach is based on the use of polarised light. Its use is not new, but apparently forgotten. Koeppe (1920) studied both normal and abnormal eyes with the polarising biomicroscope in considerable detail, but appears to have overlooked the fact that it enables one to enhance the signal-to-noise ratio in the visualization of cataracts, a matter to be dealt with elsewhere (Weale 1986). This paper confines itself to some aspects of the second of the above problems, namely that relating to the appearance of the normal lens in the slit-lamp.

The rationale is as follows. If light is passed through a polarizer P and then through an analyzer A, their two axes crossing each other, extinction of the light occurs. If, however, a diffuser such as ground glass G is interposed between P and A, extinction is partly or wholly counteracted by virtue of the light polarized by P being partly or wholly depolarized by G. If the crystalline lens acts like G, and a crossed-polarizing system is used with a slit-lamp, the appearance of the lens will remain bright. Conversely, if it were to appear dark, the presence of significant light scatter would have to be called into question.

Theory

Symbols to be used below are defined as follows:

Radiation incident on lens	$I(i, \lambda)$
Sensitivity of detector	$S(\lambda)$
Fraction of light scattered in a given direction	$s(\lambda)$
Transmissivity of the scattering medium under the experimental conditions	$T(c, \lambda)$
Width of nominally monochromatic wavelength band	$\Delta\lambda$
Measured scattering fraction	$\mathfrak{S}(\lambda)$

The response of a detector of radiation varies with the intensity and spectral composition of the radiation incident on it, and its own sensitivity (defined in terms of the radiation). When the radiation is not approximately monochromatic, then the spectral functions of the first four variables above have each to be expressed in terms appropriate to narrow wavelength bands $\Delta\lambda$. For a given wavelength λ, the functions within $\Delta\lambda$ are multiplied with one another as shown below, and summation is carried out for the spectral range under consideration, lying, say, between wavelengths $\lambda(m)$ and $\lambda(y)$.

The instrument response for the incident radiation is given by

$$R(i) = \sum_{m}^{y} S(\lambda) \cdot I(i, \lambda) \cdot \Delta\lambda,$$

that for the scattered radiation

$$R(s) = \sum_{m}^{y} S(\lambda) \cdot I(i, \lambda) \cdot s(\lambda) \cdot T(c, \lambda) \cdot \Delta \lambda l,$$

so that the measured scattering fraction becomes

$$\mathfrak{S}(\lambda) = \frac{\sum_{m}^{y} S(\lambda) \cdot I(i, \lambda) \cdot s(\lambda) \cdot T(c, \lambda) \cdot \Delta \lambda}{\sum_{m}^{y} S(\lambda) \cdot I(i, \lambda) \cdot \Delta \lambda} \tag{1}$$

When we are dealing with approximately monochromatic light, Eq. (1) simplifies to

$$\mathfrak{S}(\lambda) = s(\lambda) \cdot T(c, \lambda) \tag{2}$$

It follows that it is impossible to obtain an absolute value for the scattering fraction without any allowance being made for $T(c, \lambda)$. In the case of the crystalline lens, it is, of course, hard to say how far a scattered beam has travelled through the lens. Generally it is short-wavelength light that is both scattered and absorbed. As a first approximation it may therefore be valid to equate $T(c, \lambda)$ with $T(\lambda)$, the transmissivity of the lens for a beam traversing it.

Since it is thought that $s(\lambda)$ increases with age (Allen and Vos 1967; Niesel et al. 1975; Sigelman et al. 1974), Eqs. (1) and (2) need careful attention. Eq. (2), the simpler of the two, shows that it is not only the value of $s(\lambda)$ that is underestimated by a neglect of T, but also its variation with age (Weale 1982). In other words, the variation of $s(\lambda)$ with age is appreciable greater than published data would lead one to believe. Moreover, since, in the past, "white" light has been used, the spectral sensitivity $S(\lambda)$ can be shown to play a significant role (cf. Eq. 1). For example, if one assumes the ages of 30 and 60 to be convenient for monitoring lenticular senescence, it is instructive to compare the relative effects of a detector with spectral properties similar to those of the human eye on the one hand and those of a blue-sensitive photographic emulsion on the other. Given a set of assumed values, if the variation with senescence is represented by the ratio

$$R = \mathfrak{S}(60)/\mathfrak{S}(30) \tag{3}$$

then $R = 3.29$ in the former case and 2.92 in the latter. Equation (1) shows that only the denominator acts as a scaling factor, not affecting R. $S(\lambda)$ in the numerator exerts a distorting function as shown above. It is, therefore, difficult to carry out meaningful comparisons between sets of data obtained by various authors.

As regards the widespread quantitative efforts now being made to characterise cataracts and their progress, it is important to demonstrate that the above considerations can be ignored if conclusions based on these efforts are to be valid. The visibility of the slit-lamp image can clearly be manipulated by a shrewd choice of the variables in Eq. (1), which determine its contrast. It can be enhanced polarimetrically by discovering to what extent, if any, scattered light is adulterated by specular reflections. This is the problem addressed here experimentally.

Subjects and methods

Apparatus

The following modifications were made to a Haag-Streit slit-lamp. A polarizer (Fig. 1) with its axis parallel to the
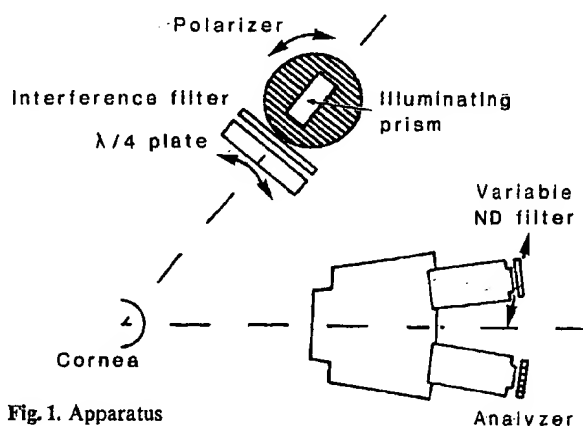

Fig. 1. Apparatus

illuminating prism of the slit-lamp was placed in front of the light source. In some instances, detailed later, an interference filter was placed in front of the prism. In front of the filter there was located a quarter-wave ($\lambda/4$)-plate. This served to compensate for any birefringence in the overall light path, including that of the cornea (Maurice 1957) and the lens (Weale 1979). One of the oculars was provided with an analyser which crossed the polarizer. The other could be covered with neutral density filters, increasing in steps of 0.1 density units.

Without the $\lambda/4$-plate, the system produced for certain angular configurations the well-known dark "Maltese Cross", due essentially to corneal birefringence. The fine cross-hatching at $\pm 45°$, described by Koeppe (1920) was also seen. The placement and rotation of the $\lambda/4$-plate causes a rotation of the arms of the cross, alternately in the same sense as, and opposite to, that of the compensator. The advantage of the rotation is that different parts of the lens can be covered in turn by an arm of the cross. It has to be emphasised that they will remain dark only in the absence of significant scattering loci. Consequently, a measurement of the apparent brightness of the cross provides a measure of the fraction of light scattered by the lens.

In the course of the experiment, the $\lambda/4$ plate was so adjusted as to maximise the luminance contrast in the centre of the lenticular nucleus, i.e. the centre was made as dark as possible. The measurement consisted in making a photometric match between this dark area and the non-analyzed image in the other ocular. The density of the analysing polaroid was ~0.7.

In theory, a $\lambda/4$ plate can be effective only for a radiation with wavelength λ. In practice, a narrow-band filter greatly reduces the luminance of the images. However, it was desirable to examine the point and accordingly the combinations shown in Table 1 were used.

The measurements outlined in the table provide no absolute value of the scattered radiation but merely the ratio of the radiation that cannot be extinguished by the analyser to the overall radiation emanating from the crystalline lens. The absolute value was determined as follows. The radiometer head of a UDT radiometer was placed against the exit aperture of the unoccluded comparison ocular. With a subject in position, a measurement was made of the radiation emerging from the ocular. The subject's eye was then replaced with a white sheet of Bristol board.
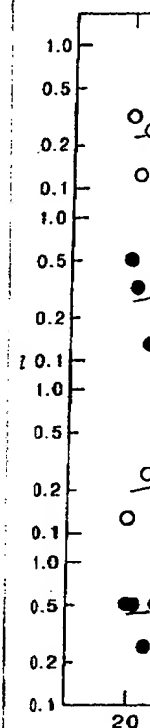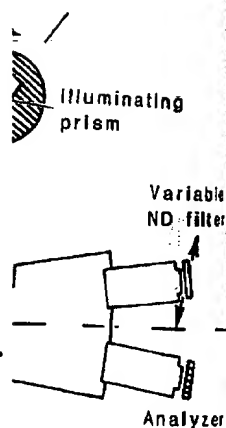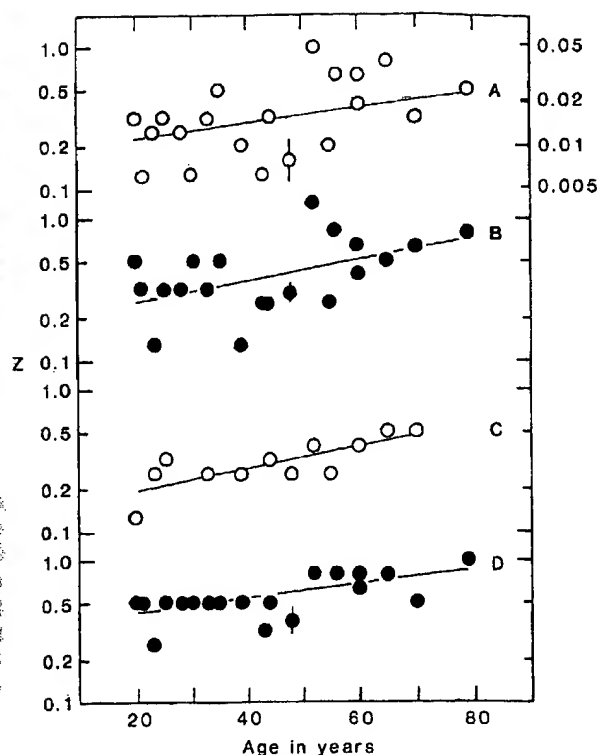
Fig. 2. *Abscissa:* age in years of subjects. *Left ordinate:* unpolarised luminous intensity of lenticular nucleus expressed as a fraction of all the light returned from it. *Right ordinate:* the left ordinate scaled to absolute values in terms of the radiation incident on the eye. For meaning of letters, see Table 1 and Results. Straight lines represent regressions

needed for an evaluation of the brightness of the lens (Weale 1985) and the scattering coefficients.

Subjects

The left eyes of 20 normal and 1 slightly cataractous subjects were studied. Ages ranged from 20 to 79 years. In general, only one measurement was made; however, as it was desirable to establish the precision of the method, several repeats were made. A typical set of measurements gave a $\sigma = 0.047$, i.e. $\pm 11\%$ for $N = 3$ (cf. Fig. 2).

Results

The experimental data are shown in Fig. 2 where the age in years is plotted along the abscissa and the unextinguished light as a fraction of the total along the left ordinate. This value is net of that of the analyser (0.7 N.D.). On the right hand side, the data are scaled to correspond to the absolute value of the scattering coefficients, as measured with white light (cf. above). The lines represent linear regressions, the equations for which are as follows:

A: $y = -0.841 + 0.00763\,x$; $r = 0.4965$; $P < 0.03$ $N = 20$

B: $y = -0.732 + 0.00717\,x$; $r = 0.4893$; $P < 0.03$ $N = 20$

C: $y = -0.863 + 0.00768\,x$; $r = 0.7608$; $P < 0.002$ $N = 14$

D: $y = -0.514 + 0.00549\,x$; $r = 0.64$; $P < 0.005$ $N = 19$

It is a moot point whether the high r-value for C is due to the $\lambda/4$ plate being appropriate for the wavelength of the incident radiation and, correspondingly, the low slope for D to the gross discrepancy shown in Table 1. Statistically, there is no difference between the four r-values.

Discussion

It is perhaps worth repeating that Fig. 2 does not show what is conventionally referred to as scattered light. It tells us about that fraction of the apparently scattered light, which is not extinguished by the analyser. (In fact, it can be shown that if the antilog of the ordinates is Z, $P/S = (1/Z) - 1$ where P is the extinguished and S the unextinguished moiety of the light coming from the illuminated lens.) This is why the title of this paper refers to real scattered light. Z increases progressively with age, but a linear extrapolation of the regression does not reach unity till beyond the ninth decade. At the age of 70 only half the light in the slit-lamp image appears to be due to scattered light; at younger ages it forms much of the minor component. It is likely that the extinguished component P follows a shorter light-path in the lens than is true of the unextinguished (scattered) moiety S. If so, then S will decrease faster with age than P with the result that P/S will increase on this account in regions of high absorbance, thereby tending to cancel the rate of decrease of this value and the consequent rate of increase of Z plotted in Fig. 2. This may explain the relatively low slope of the regression for D above.

The similarity between the four regressions suggests that long-wavelength light (which is strongly present in A) does not significantly contribute to the scattering fraction s (cf. Weale 1983). This provides an independent explanation of why the image-forming capacity of the crystalline lens, as measured with blue-free light, remains virtually

Table 1. Filters and $\lambda/4$-plate combinations

| | Condition | Spectral distribution of incident radiation | | | |
		A	B	C	D
Quarter wave plate	470 nm/4 529 nm/4		white	485 nm[a]	470 nm[c] 415 nm[b]

[a] Manufacturer's data (glass filter BG 39)
[b] Manufacturer's data (glass filter BG 39)
[c] Calibrated interference filter BG 12

The above measurement was repeated. In addition, the radiometer head was placed in front of the ocular with the white sheet in position. These measurements made it possible to calculate the illumination in front of the ocular due to light scattered by the lens. Finally, the radiometer head was placed in the plane of the slit, perpendicularly to the illuminating beam. The sensitivity of the radiometer was inadequate for an extension of this measurement to monochromatic radiations. However, since it was desirable merely to determine the order of the magnitude so as to arrive at a comparison with earlier work, this was not considered a severe drawback. An estimate of the area of the beam was obtained, as was one of the area of crystalline lens illuminating the radiometer. These quantities are

(left margin fragments, partially legible:)

Illuminating prism

Variable ND filter

Analyzer

...mp was placed in front... ...es, detailed later, an int... ...t of the prism. In front... ...arter-wave ($\lambda/4$)-plate. T... ...irefringence in the over... ...cornea (Maurice 1957) a... ...the oculars was provi... ...the polarizer. The oth... ...ensity filters, increasing...

...stem produced for certain... ...ll-known dark "Malte... ...al birefringence. The fir... ...ed by Koeppe (1920) wa... ...rotation of the $\lambda/4$-pla... ...f the cross, alternately a... ...to, that of the compens... ...on is that different part... ...n by an arm of the cros... ...ey will remain dark only... ...tering loci. Consequently... ...ightness of the cross pro... ...of light scattered by the...

...nt, the $\lambda/4$ plate was so... ...minance contrast in the... ...i.e. the centre was made... ...nent consisted in making... ...; dark area and the non... ...r. The density of the ana...

...ffective only for a radia... ...ce, a narrow-band filter... ...the images. However, it... ...int and accordingly the... ...re used.

...n the table provide no... ...adiation but merely the... ...be extinguished by the... ...manating from the crys... ...s determined as follows... ...radiometer was placed... ...occluded comparison oc... ...measurement was made... ...ie ocular. The subject's... ...sheet of Bristol board.

optimal throughout life. However, this conclusion is tentative in the sense that data obtained with white light have to be treated with particular caution, as suggested in the section on theory.

The absolute values (Fig. 2, right-hand scale) are comparable with those due to Allen and Vos (1967), even though somewhat different techniques were employed in the two studies, and there is also a difference in the underlying photometry.

With the above demonstration that throughout most of our life the major portion of the light "scattered" by the lens is very likely to arise from apparently specular reflections, one naturally asks about the underlying mechanism. The lens is made up of layers, the number of which increase throughout life. Such layers can reflect light only if their refractive index differs from that of their environment. The thickness of the layers is also significant. At 2.5–3 μm, the diameter of the nuclear layers is a relatively small multiple of the wavelength, and interference effects may be imagined as taking place. Goldmann (1937) has shown that the number of disjunction stripes increases with age and Niesel et al. (1976) have reported a decrease in their size. In addition, Hayes and Fisher (1984) have described a mechanism underlying polychromatic lustre in a case of Christmas-tree cataract. At this stage, it is not feasible to plump for any one of this plethora of possible explanations or others based on the relative importance of density and orientation fluctuations. Suffice it to say that multiple reflections are conceivable, but that an elucidation of the underlying mechanism will require a more detailed experimental approach.

It is unlikely that the amount of real scatter is reduced in lenses classed as cataractous, but the reverse of the problem, namely whether they exhibit any extinguishable light, is of considerable practical interest. If the answer is "yes", then it is probable that opacities can be visualised more easily and earlier and in more detail than heretofore. This problem is considered separately (Weale 1986).

References

Allen MJ, Vos JJ (1967) Ocular scattered light and visual performance as a function of age. Am J Optom Physiol Opt 44:717–727

Campbell FW, Robson JG (1968) Application of Fourier analysis to the visibility of gratings. J Physiol 197:551–566

Flamant F (1955) Étude de la répartition de lumière dans l'image rétinienne d'une fente. Rev Opt Theor Instrum 34:433–459

Goldmann H (1937) Studien über die Alterskernstreifen der Linse. Arch Augenheilkd 110:405–414

Hayes BP, Fisher RF (1984) Ultrastructural appearances of a lens with marked polychromatic lustre: evidence for diffraction as a cause. Br J Ophthalmol 68:850–858

Koeppe L (1920) Das biophysikalisch-histologische Verhalten der lebenden Augengewebe unter normalen und pathologischen Bedingungen im polarisierten Lichte der Gullstrandschen Nernstspaltlampe. Graefes Arch Clin Exp Ophthalmol 102:4–97

Lerman S, Hockwin O (1985) Automated biometry and densitography of anterior segment of the eye. Graefes Arch Clin Exp Ophthalmol 223:121–129

Maurice DM (1957) The structure and transparency of the cornea. J Physiol 136:263–286

Niesel P, Kräuchi H, Bachmann E (1976) Der Abspaltungsstreifen in der Spaltlampenphotographie der alternden Linse. Graefes Arch Clin Exp Ophthalmol 199:11–20

Sigelman J, Trokel SL, Spector A (1974) Quantitative biomicroscopy of lens light back scatter. Arch Ophthalmol 92:437–442

Weale RA (1979) Sex, age and the birefringence of the human crystalline lens. Exp Eye Res 29:449–461

Weale RA (1982) A biography of the eye – development, growth, age. H.K. Lewis, London

Weale RA (1983) Transparency and power of post-mortem human lenses: variation with age and sex. Exp Eye Res 36:731–741

Weale RA (1985) Human lenticular fluorescence and transmissivity, and their effects on vision. Exp Eye Res 41:457–473

Weale RA (1986) A new method for visualising discontinuities in the crystalline lens. Br J Ophthalmol (in press)

Zuckerman JL, Miller D, Dyes W, Keller M (1973) Degradation of vision through a simulated cataract. Invest Opthalmol 12:213–224

SEP 28, 2004

FILLED SEP 2 8 2004

DOCLINE: Journal   Copy   Epayment

Title:	Graefes archive for clinical and experimental ophthalmology = Albrecht von Graefes Archiv für klinis
Title Abbrev:	Graefes Arch Clin Exp Ophthalmol
Citation:	1986;224(5):463-6
Article:	Real light scatter in the human crystalline lens.
Author:	Weale RA
NLM Unique ID:	8205248 Verify: PubMed
PubMed UI:	3758692
ISSN:	0721-832X (Print)
Publisher:	Springer Verlag, Berlin
Copyright:	Copyright Compliance Guidelines
Authorization:	romero
Need By:	N/A
Maximum Cost:	$18.00
Patron Name:	
Library Groups:	RESOURCE,EFTS,SCAMeL
Phone:	1.505.272-8052
Fax:	1.505.272-5350
Email:	docdel@salud.unm.edu
Comments:	**Ariel Preferred or Mail. EFTS. We use ARIEL 3.3**
Routing Reason:	Routed to TXUTTU in Serial Routing - cell 1
Received:	Sep 28, 2004 (04:36 PM EST)
Lender:	Texas Tech University Health Sciences Center/ Lubbock/ TX USA (TXUTTU)

Bill to: NMUMEX